LOW TEMPERATURE THERMAL CONDUCTIVITY OF LIGHTLY DOPED $KMgF_3:Cr^{2+}$

By

HADI SALAMATI-MASHHAD

Licentiate

University of Mashhad

Mashhad-Iran

1972

Submitted to the Faculty of the Graduate College
of the Oklahoma State University
in partial fulfillment of the requirements
for the Degree of
MASTER OF SCIENCE
July, 1977

LOW TEMPERATURE THERMAL CONDUCTIVITY OF

LIGHTLY DOPED $KMgF_3:Cr^{2+}$

Thesis Approved:

George S. Dixon
Thesis Adviser

Joel J. Martin

Larry E. Halliburton

Norman N. Durham
Dean of the Graduate College

ACKNOWLEDGMENTS

The author wishes to express his appreciation to his major advisor, Professor George S. Dixon, for his guidance and assistance throughout this study, as well as his encouragement and kind friendship shown during the author's stay at Oklahoma State University.

Appreciation is also expressed to Professor J. J. Martin for letting us use his laboratory and his assistance.

TABLE OF CONTENTS

LIST OF TABLES

LIST OF FIGURES

CHAPTER I

INTRODUCTION

Purpose of This Investigation

Thermal conductivity measurements of pure and chromous-doped potassium magnesium fluoride were performed by López (1). López observed Cr^{2+} resonances in potassium magnesium fluoride, but at the high doping levels used, the transition from ground state in this model was obscured by point defect scattering. This study was made at a much lower doping level to test the model proposed by López from observations of the resonant scattering associated with transition from ground state.

Resonant Scattering From Paramagnetic Defect

There are several experimental methods to study the interaction between a paramagnetic ion and vibrations of the lattice. One of these methods is thermal conductivity, which in a paramagnetic crystal is affected by average interaction of the thermal phonon with the magnetic ions.

In an insulating paramagnetic crystal at low temperature only the lowest energy levels of the magnetic ions are populated. The thermal conductivity can be expressed as the sum of contribution from phonons of different energy. If the difference in energy between a pair of low-lying energy levels happens to be comparable to the energy of the dominant phonons then phonons may induce transitions in the magnetic ions.

Because of their absorption and subsequent re-emission in random direction, the phonons will themselves be scattered. This causes a reduction of their contribution to the heat flow and in thermal conductivity of the specimen. The phonons which are at resonance with the energy levels of the magnetic ions would not participate to the heat current (2,3).

Cr^{2+} in Octahedral Site

The electronic structure of Cr^{2+} is $3d^4$. In a cubic crystal, such as $KMgF_3$ it interacts with the lattice through the octahedral electric field of the surrounding ions.

In an octahedral site the ground state orbital level should be E^5. However, the Jahn-Teller theorem indicates that the orbital degeneracy will be removed by spontaneous lower symmetry distortion of surroundings (4). As a result of the Jahn-Teller effect in octahedral symmetry for chromous ion and nearest neighbor octahedral symmetry for the chromous ion and nearest neighbor octahedrals, one would expect resonant scattering of phonons from the vibronic states of the complex. The Fletcher and Stevens (5) model which was used by López (1) developed a model for the dynamic Jahn-Teller effect of octahedrally coordinated $3d^4$ ion. According to this model the ground state of a $3d^4$ ion split into seven energy levels A_1, A_2, E_1, E_2, T_1, T_2 and T_2'. By selection rules following from group theory, only eight transitions are allowed. E_2-A_1, E_1-A_1, A_2-E_2, E_1-E_2, E_1-A_2, T_2'-T_1, T_2-T_1 and T_2-T_2'. As already explained by López (1), the energy levels depend on two parameters: δ the tunneling frequency and D the spin-orbit coupling. The expressions for the energy levels and the values found by López are given in Appendix B.

CHAPTER II

EXPERIMENTAL METHOD

Potassium magnesium trifluoride is a cubic perovskite insulator. It has one molecule per unit cell and lattice constant of a = 3.973$\mathring{A}$ (6). Its elastic constants C_{11}, C_{12}, C_{44} have been determined from ultrasonic experiments (7).

The calculated elastic constants are

$$C_{11} = (132.0 \pm 1.5) \times 10^{10} \quad \text{dyne/cm}^2$$

$$C_{12} = (39.6 \pm 1.5) \times 10^{19} \quad \text{dyne/cm}^2$$

$$C_{44} = (48.5 \pm 0.6) \times 10^{10} \quad \text{dyne/cm}^2$$

the average velocity of sound is 4.77×10^5 cm/sec (8), and its density is 3.17 ± 0.01 gm/cm^3. The structure of potassium magnesium trifluoride is shown in Figure 1.

The chromous doped sample of potassium magnesium fluoride was grown in the Oklahoma State University Crystal Growth Laboratory from stoichiometric mixtures of KF and MgF_2 by a Bridgman-Stockbarger technique. Dopant Cr was added by adding CrF_2 to the melt. Details about the growth apparatus and procedure are given by Wolf (9).

Preparation of Sample

The sample was cut into a parallelepiped of the dimension given in

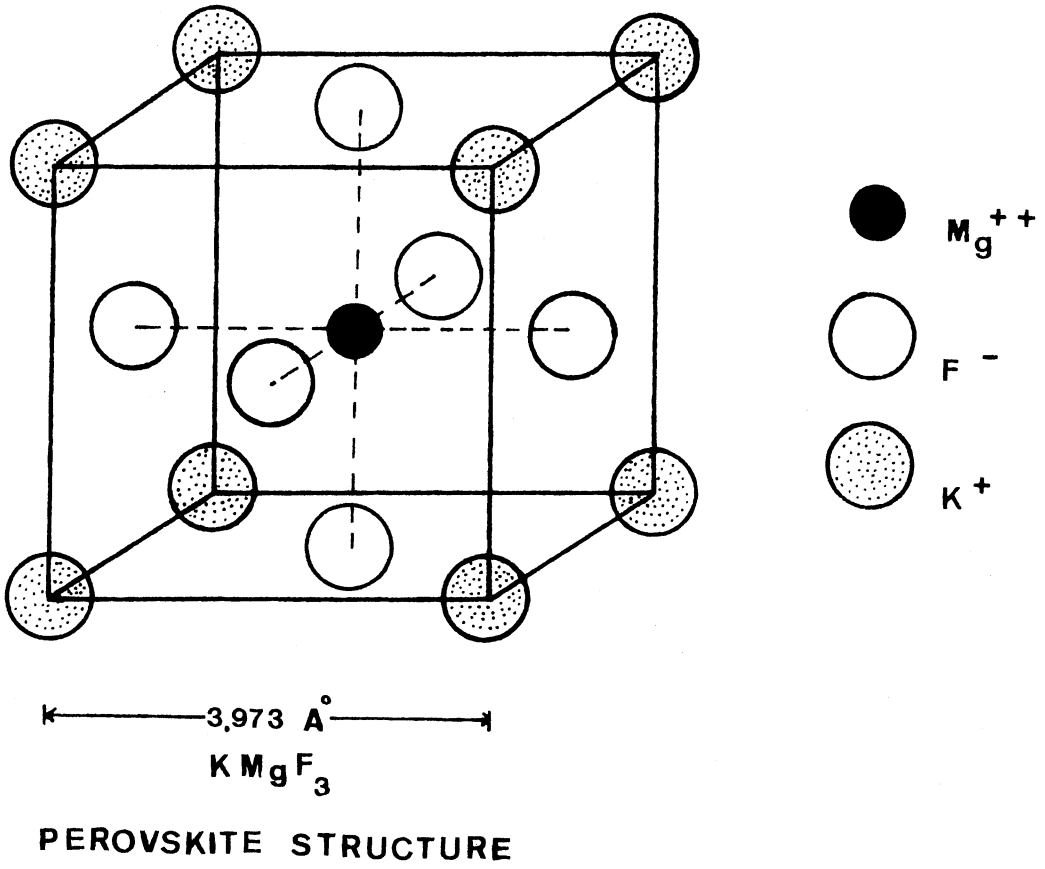

Figure 1. Crystal Structure of Potassium Magnesium Fluoride

Table I. The concentration of chromous impurities in potassium magnesium fluoride was smaller than the samples were used by López (1).

TABLE I

DIMENSION OF THE SAMPLE

Sample	Length (mm)	Width (mm)	Height (mm)	Orientation
$KMgF_3$ Cr-doped	14.01	2.55	2.64	[100]

Experimental Determination of Thermal Conductivity

In this experiment the measurement was made by the method of steady-state flow. For a steady-state flow of heat through a solid having a temperature gradient ∇T, the thermal conductivity, λ, is defined by the relation

$$\vec{Q} = - \lambda \vec{\nabla T} \tag{1}$$

where Q is the energy transmitted across unit area per unit time. In the special case of a long, rod-shaped solid having uniform cross-sectional area, A, with heat flow along the long axis of the sample, Equation (1) becomes

$$\frac{P}{A} = \lambda \frac{\Delta T}{\Delta X} \tag{2}$$

where P is the power supplied to one end of the sample and ΔX is dis-

tance between which the change in temperature ΔT is measured. To calculate the thermal conductivity from the experimental data where the input power is known, one experimentally measures the temperature difference ΔT and from the dimensions of the sample's cross-sectional area, A, and thermometer separation, L, determines the geometrical factor L/A. Equation (2) is solved to give the thermal conductivity by

$$\lambda = (L/A) \frac{P}{\Delta T} \tag{3}$$

Apparatus

For the range of interest 2.6 to 28K in which the measurement were performed, the same apparatus was used, which were used by López (1), Wolf (9) and Velasco (10). This apparatus is described in considerable detail by Velasco (10); therefore only a brief description will be given here.

Figure 2 shows a schematic of the sample holder. The sample was mounted at the end of a copper rod was constructed so that the effective thermal contact with the cryogenic liquid bath, either liquid helium-4 or liquid nitrogen, could be controlled by controlling the pressure of helium gas in the heat leak chamber. When helium gas was put into this chamber, the thermal contact with the cryogenic bath was good, giving the copper rod the same temperature as the bath. If the sample was heated and transmitted heat to the copper rod, or if a current was passed through the 100 ohm ambient heater wrapped around the copper rod, the heat was quickly dissipated into the bath, approximately maintaining the bath temperature. If the thermal contact between the copper heat sink and the cryogenic bath was reduced by pumping some of the

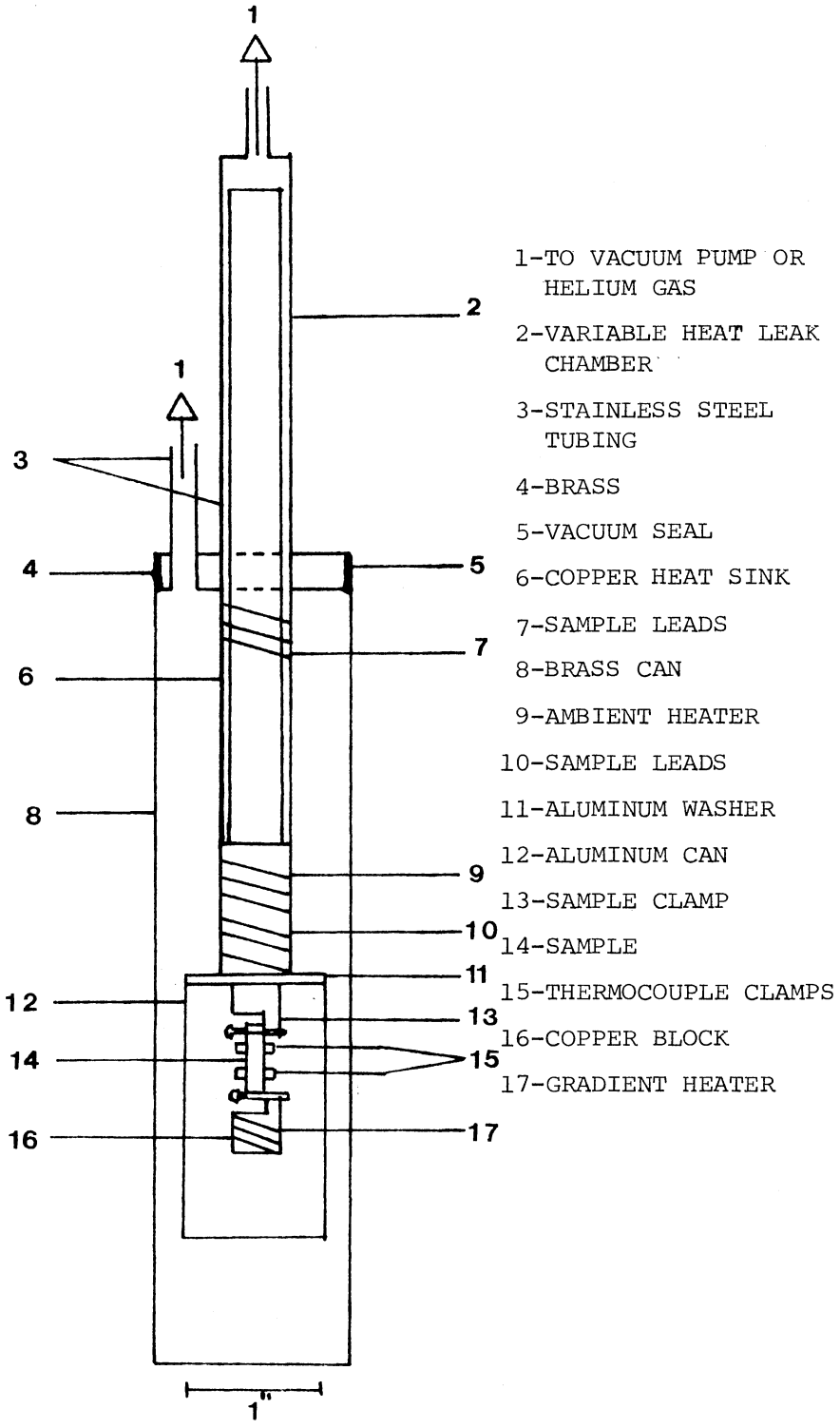

Figure 2. Thermal Conductivity Sample Holder

helium gas out of the heat leak chamber, then the heat dissipated to the copper heat sink was not removed efficiently and raised the temperature of the heat sink and the sample. With a good vacuum in the heat leak chamber, the heat sink was effectively isolated from cryogenic bath, therefore, the temperatures were much higher than the bath's could be reached.

If the cryogenic liquid was helium at 4.2K, temperatures as high as 50K could be reached with less than 250 milliwatts of input power. If liquid nitrogen at 77K was the cryogenic liquid, temperatures above 200K could be obtained with approximately one watt of input power. At the higher temperatures, radiation heat loss became a large source of error when the sample temperature was greatly different from that of the outer wall of the sample holder. For reduction of this radiation loss, an aluminum heat shield was placed around the sample, its clamps and gradient heater. This aluminum shield was therefore kept at approximately its temperature, greatly reducing the temperature difference between the sample and surroundings.

The entire assembly described above was enclosed in a brass can which was then submerged into the cryogenic fluid. When measurements were being taken, a vacuum of less than 10^{-5} Torr was maintained inside the brass can, thus insuring proper temperature and heat loss control.

The sample was held in thermal contact with the heat sink by a copper clamp containing indium pads which flattened against the sample when the nylon screws were tightened. A phosphor bronze spring and the nylon screws compensated for the difference in the thermal expansion between the sample and the clamp. The two thermometer clamps were constructed in a similar manner.

The temperature gradient in the sample was established by a heater clamp onto the end of the sample farthest from the heat sink. Current was supplied to the heater by #40 copper wire, and the voltage drop across the heater was measured through #36 constantan wire.

The thermometers used in this apparatus were chromel versus gold 0.07 atomic percent iron. They were soldered to the clamps with indium solder. The emf of T and ΔT were read using a potentiometer. The potentiometer used to measure T was a Leeds and Northrup Type K-3 universal potentiometer in series with a Model 2770 Honeywell potentiometer with a Leeds and Northrup 9838 guaded nanovolt detector as a null indicator, thus allowing the emf to be resolved to the nearest 0.1 microvolt. The Honeywell potentiometer and nanovolt detector were used for measuring ΔT with a 0.01 microvolt resolution. The gradient heater voltage and current were monitored on a Triplett D.C. millivolt digital panel meter, giving accuracy to three or four significant figures, depending on the magnitude of the current supplied to the heater. A stable current to the gradient heater was delivered by a regulated power supply.

All of the leads leaving into and out of the sample holder were thermally anchored to the copper heat sink with GE-7031 varnish.

Errors

Measurement Errors

The errors in the thermal conductivity calculations made using Equation (3) dependent on the absolute and relative percision in the measurements of the sample cross section, input power, sample temperature, and gradient temperature.

The dimensions used to calculate the cross-sectional area, A, were measured with a micrometer to the nearest 0.01 mm. Since the sample was not a perfect parallele piped, each end was measured with the average values used in the calculation.

The measurement of the thermometer spacing clamp was the most uncertain measurement taken. The clamp separation, L, was determined by placing a spacer, whose thickness was measured with a micrometer, between the inner edge of one clamp and the outer one of the other clamp.

The power input to the hot end of the sample was determined by measuring the current through the gradient heater. The current I was determined by measuring the voltage drop across a 10 ohm standard resistor. This current was read to four figures with uncertainty of ±3 in the last digit. The input power was calculated using P = VI, and the voltage V was read directly from the digital millivoltmeter.

Heat Loss Errors

In using the Equation (3) we assumed that all the power that was converted to heat that flowed uniformly through the sample.

Since the sample was in the vacuum of better than 10^{-5} Torr, convection and conduction of the heat directly from the sample to the wall of the sample holder could be ruled out as dissipating heat. Conduction through the wire leads going into the sample chamber, was analyzed in detail by Wolf (9) and dissipation of heat due to conduction was found to be negligible.

In term of the radiation heat loss, $Q_{radiation}$, is approximated by

$$Q_{radiation} = 4\, a'\, \sigma\, E\, T^3 \Delta T$$

where a' is the surface area of the sample, σ is the Stefan-Boltzmann constant, E is the emissivity of the sample, This the temperature, and ΔT is the difference between the sample's temperature and the chamber wall's temperature.

Because of special interest, the measurement was made at low temperature, so the radiation heat loss was negligible. Of course, at high temperature it could become quite significant.

CHAPTER III

EXPERIMENTAL RESULTS

The thermal conductivity of chromous-doped sample of potassium magnesium fluoride single crystal was measured from 2.6 to 28K.

In the peak region between 15 and 20K, the thermal conductivity is approximately 6 W/cmK less than undoped sample (comparing with López's data (1) for undoped sample). Below 4K the thermal conductivity curve had a slope of approximately T^3.

Figure 3 gives the thermal conductivity data for Cr-doped potassium magnesium fluoride.

The resonances near 4K and 6K as observed by López, seems to be existent and an additional resonance near 10K, which is interpreted as evidence of third frequency resonance.

A tabulation of all data points taken is presented in Appendix A.

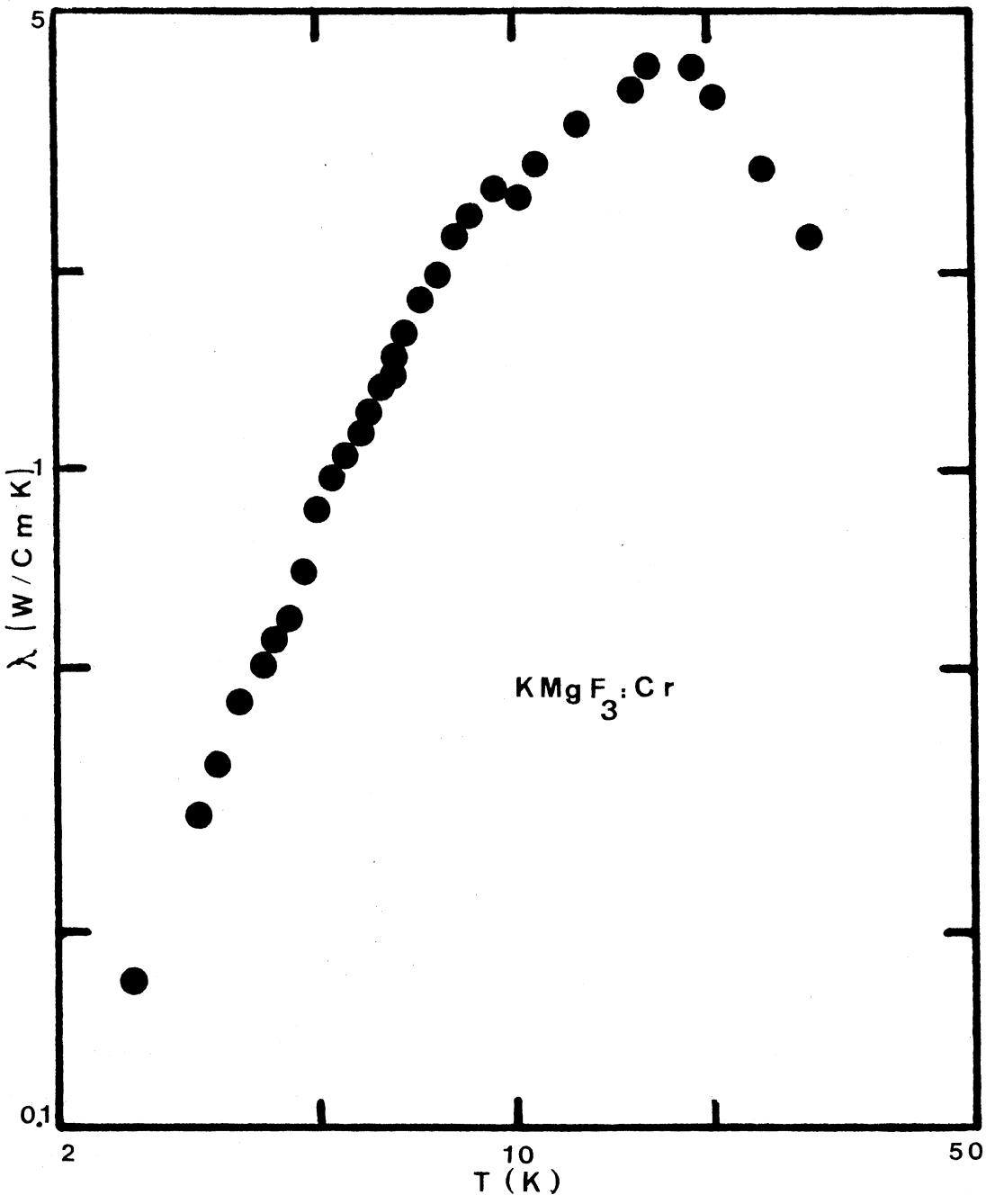

Figure 3. Thermal Conductivity of the Cr-Doped KMF_3

CHAPTER IV

ANALYSIS AND DISCUSSION

Debye-Callaway Model

The use of thermal conductivity in the spectroscopic examination of impurities in crystal is a consequence of the fact that in the Debye approximation the thermal conductivity is proportional to a known weighted average of the total phonon relaxation time $\tau(\omega,T)$, which in turn depends on the nature and concentration of the impurities present. The conductivity is given by the expression

$$\lambda(T) = \frac{k}{2\pi^2 v}\left(\frac{kT}{\hbar}\right)^3 \int_0^{\theta/T} \frac{x^4 e^x}{(e^x-1)^2}\,\tau(x,T)\,dx \qquad (4)$$

$$\left(x = \frac{\hbar\omega}{kT}\right)$$

where v is the velocity of sound assumed constant, $\tau(\omega,T)$ is phonon relaxation time, θ the Debye temperature and the other samples have their usual meaning.

Previous experiments have successfully tested the Debye-Callaway model of thermal conductivity (4,11,12).

The major contribution of Callaway's treatment is the reciprocal addition of all the relaxation times to get one total relaxation time τ_{total}

$$\tau_{total}^{-1} = \Sigma_i \tau_i^{-1} \quad (5)$$

where τ_i are relaxation times describing the individual scattering sources.

Discussion

Using Equation (5) in Equation (4) to obtain a computer fit of the thermal conductivity experimental data for the pure sample by López, the best fitting was obtained by assuming three relaxation times, boundary, isotope, and phonon-phonon, so that the total relaxation time becomes

$$\tau_{total}^{-1} = \tau_{boundary}^{-1} + \tau_{isotope}^{-1} + \tau_{phonon\text{-}phonon}^{-1} \quad (6)$$

Casimir (13) first derived the relaxation time resulting from diffuse boundary scattering as

$$\tau^{-1} = \frac{V}{L} \quad (7)$$

where V is the velocity of sound in the crystal and L is an effective sample diameter which is dependent upon the sample's geometry and surface roughness. For a "perfectly rough" and rectangular sample,

$$L = 2\pi^{-\frac{1}{2}} [\ell_1 \ell_2]^{\frac{1}{2}} \quad (8)$$

where ℓ_1 and ℓ_2 are the dimensions of the sample cross-section perpendicular to the heat flow with the assumption that the crystal is long compared to either ℓ_1 or ℓ_2.

As the temperature of crystal decreases, the importance of the long wavelength phonons increases. At low enough temperatures, when all

the phonon mean-free-path are comparable to the sample's cross-sectional dimensions, the relaxation time is usually entirely limited by the boundary which is temperature and frequency independent.

The thermal conductivity curve for these temperatures will have a slope of T^3 resulting from the temperature dependence of the specific heat.

The effective Casimir length for sample is given in Table II.

TABLE II

CALCULATED CASIMIR LENGTH FOR SAMPLE

Sample	Effective Casimir Length (cm)
$KMgF_3:Cr^{2+}$	0.293

Point defect scattering relaxation time, τ_{PD}, was estimated for the effective of isotopes by using the relation found by Klemens (14), result in a Rayleigh-type scattering of the phonon. This relaxation time is

$$\tau_{PD} = A\omega^4 \tag{9}$$

where

$$A = \frac{\delta^3 \Gamma}{4\pi v^2} \tag{10}$$

where δ is the cube root of the atomic volume, v is the velocity of sound in the material. The form of Γ have been suggested by Slack (15). It may be applied to compounds containing isotopes of many elements. For a compound with general form A_x, A_y, A_z,...we have

$$\Gamma = \Sigma \frac{x}{x+y+z+\cdots} \left(\frac{M_A}{\bar{M}}\right) \Gamma_A + \frac{y}{x+y+z+\cdots} \left(\frac{M_B}{\bar{M}}\right) \Gamma_B + \cdots \qquad (11)$$

where

$$\Gamma_A = \sum_i f_i \left(\frac{\Delta M_i}{\bar{M}_A}\right), \cdots \qquad (12)$$

M_A and M_B are the masses of the isotopes of the atoms of types A and B respectively, $\bar{M}_A$ and $\bar{M}_B$ are the average masses of these atoms, and $\bar{M}$ is the average molecular mass defined as

$$\bar{M} = \frac{x\,\bar{M}_A + y\,\bar{M}_B + \cdots}{x + y + \cdots} \qquad (13)$$

f_i is the fractional concentration of the ith isotope and ΔM_i is the difference between atomic mass of the ith point isotope and the average atomic mass.

The approximation value of A have been calculated by López (1) was 1.13×10^{-44}.

The relaxation time, t_{pp}, resulting from the phonon-phonon process (16) was

$$\tau_{pp}^{-1} = (B_N + B_u\, e^{-\theta/aT})\, \omega^2 T \qquad (14)$$

With the aid of an electronic computer and the relaxation time

$$\tau^{-1} = \frac{v}{L} + A\omega^4 + (B_N + B_u e^{-\theta/aT})\ \omega^2 T \qquad (15)$$

a good fit of the thermal conductivities data was obtained for pure sample by López (1).

The thermal conductivity of lightly chromous doped sample was slightly higher than the chromous doped sample was used by López (1). Figure 3 shows the two resonance near 4K and 6K as observed by López, and in addition a shoulder about 9K as well as a plateau about 10K. This reduction of thermal conductivity interpreted as indicating a third scattering resonance about 10K.

To account for the data on the chromous doped sample a total relaxation time of the form

$$\tau^{-1} = \tau_p^{-1} + \Delta A\ \omega^4 + \tau_R^{-1} \qquad (16)$$

was used. τ_p is the relaxation time found for the undoped sample. The $\Delta A\ \omega^4$ is included for the increased Rayleigh scattering expected from the Cr impurities, and τ_R is the resonance relaxation time.

The relaxation time was proposed by Pohl and co-workers to account for resonances due to tunneling defects (17) were used

$$\tau_R^{-1} = \frac{B_1\omega^2}{(\omega_{01}^2-\omega^2)^2} + \frac{B_2\omega^2}{(\omega_{02}^2-\omega^2)^2} + \frac{B_3\omega^2}{(\omega_{03}^2-\omega^2)^2} \qquad (17)$$

In using the above expression, we have been considering the following criteria.

1. The resonance term should reproduce the experimental data as closely as possible.

2. The strength of the scattering (B) should scale with the Cr concentration of the sample.

3. The number of unknown parameters in the resonance terms should be kept to a minimum.

4. The resonant frequencies should be those calculated by López from his experimental data.

So, by adjusting scattering strengths (B), but not the resonant frequencies, a good fit of the thermal conductivities data was obtained for the sample. A plot of the experimental and fitted data for the sample appears in Figure 4.

It was found that the two transition $E_1 \rightarrow A_2$ and $E_1 \rightarrow E_2$ which were observed by López (1) occur again as expected. In addition a third transition $E_1 \rightarrow A_1$ in the energy level scheme of López as shown in Figure 5 is needed to reproduce the resonance at ~ 10K.

At the lowest temperatures the fit to the data is rather poor. This may result from additional scattering by the $E_2 \rightarrow A_1$ transition shown by the dashed line in Figure 5 or by scattering from other impurities that may be important at this low level of doping.

Summary and Conclusions

The thermal conductivity of chromous-doped sample of potassium magnesium fluoride were measured over the temperature range from 2.6 to 28K.

The result were analyzed in terms of Debye-Callaway model.

In addition to the two resonances observed by López, a third transition scattering at higher temperatures was observed. The frequency required to reproduce the data is consistent with the $E_1 \rightarrow A_1$ transition

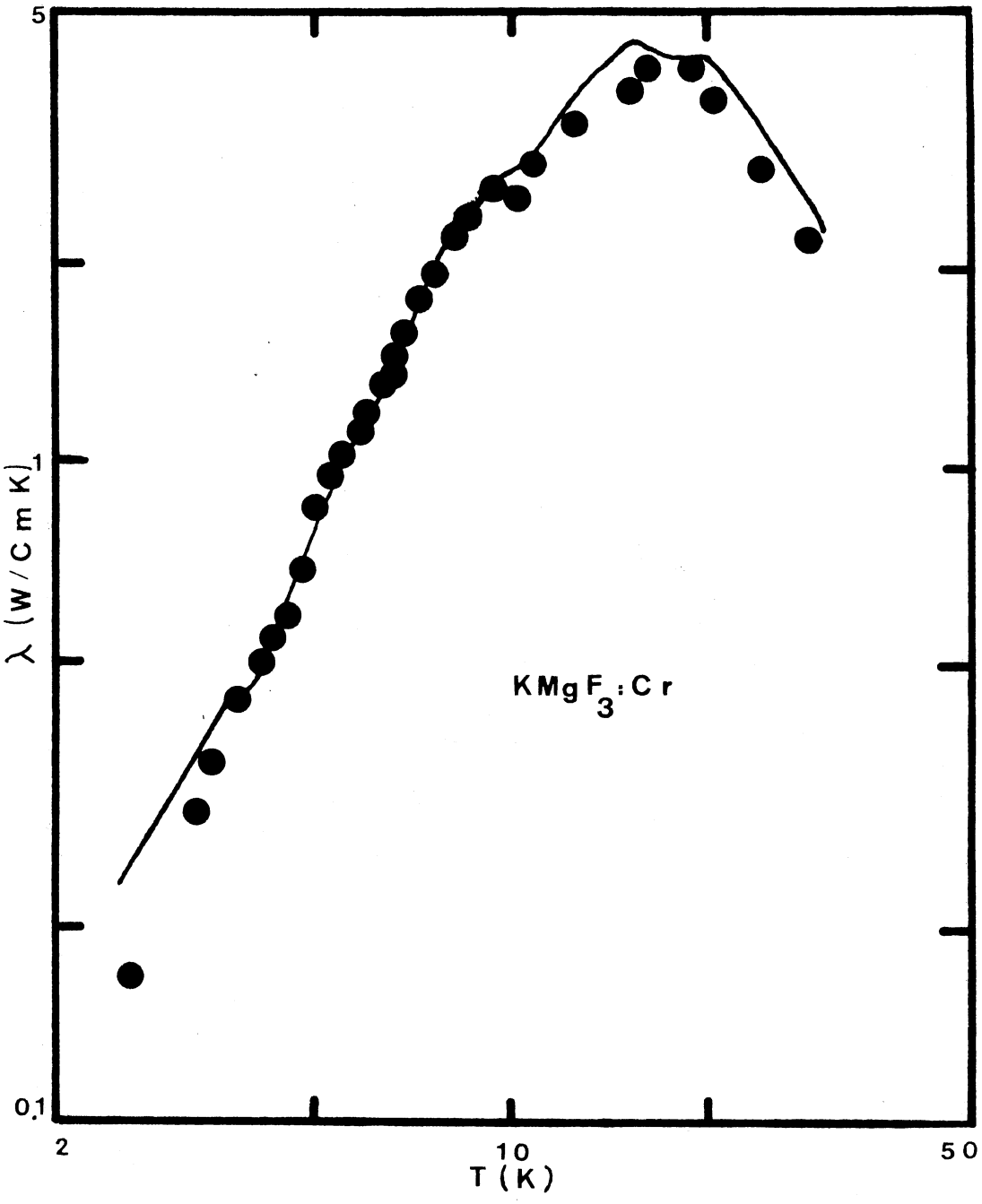

Figure 4. A Comparation of the Measured Thermal Conductivities of Cr-Doped $KMgF_3$ With Theoretical Curve Calculated From the Callaway Model

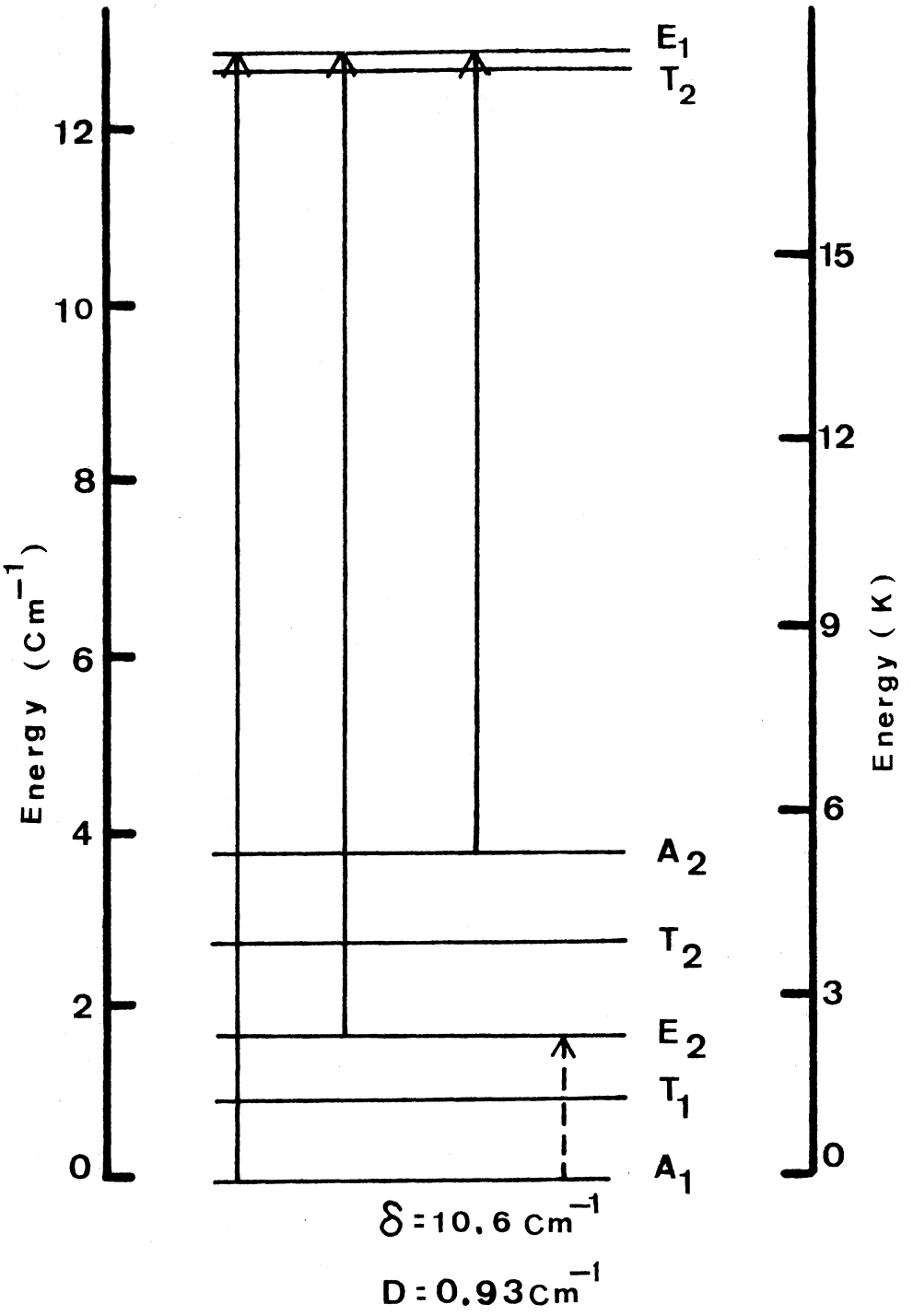

Figure 5. Energy Level Diagram for Cr^{2+} in $KMgF_3$ Including the Jahn-Teller Effect

from the ground state in López's model and tends to confirm the validity of his energy level scheme.

More work at lower temperatures and in magnetic field is needed to fully understand the scattering processes.

BIBLIOGRAPHY

1. López, Augusto R., "Low Temperature Thermal Conductivity of $KMgF_3$: Cr^{2+}" (Unpublished Ph.D. Dissertation, Oklahoma State University, 1976).

2. Walker, C. T. and R. O. Pohl, "Phonon Scattering by Point Defect" (Phys. Rev. 131 (1963) 1433-1442).

3. Walton, D., "Phonon Scattering by Paramagnetic Ions and Scattering by Other Defects," Phys. Rev. 151 (1966), 627-628.

4. Challis, L. J., et al., "In Investigation of the Ground State of Cr^{2+} in MgO Based on Thermal Conductivity Measurements," Proc. R. Soc. Lond. A 330 (1972) 92-58.

5. Fletcher, J. R. and K. W. H. Stevens, "The Jahn-Teller Effect of Octahedrally Co-ordinated $3d^4$ Ions," J. Phys. C., 2 (1969) 444-456.

6. Wychoff, R. W. G., Crystal Structures, Vol. 2, Ed. Interscience Publishers, New York, John Wiley & Sons, 1967.

7. Rosenberg, H. M. and J. K. Wigmore, "The Elastic Constant of Potassium Magnesium Fluoride," Phys. Lett., Vol. 24A (1967) 317.

8. Harley, R. T. and H. M. Rosenberg, "The Thermal Conductivity of Ni^{2+} Doped $KMgF_3$ in a Magnetic Field at Low Temperatures: The Effect of Single Ions and Coupled Pairs." Proc. Soc. Lond. A 315 (1970), 551-569.

9. Wolf, Michael W., "The Low Temperature Thermal Conductivity of Potassium Zinc Fluoride" (Unpublished Ph.D. Dissertation, Oklahoma State University, 1974).

10. Velasco, P. P. (Unpublished M.S. Thesis, Oklahoma State University, 1973).

11. Callaway, Joseph. "Model for Lattice Thermal Conductivity at Low Temperature." Phys. Rev. 113 (1959), 1046-1051.

12. Challis, L. J., M. A. McConachie, and D. J. Williams. "An Investigation of Phonon Scattering by Chromous Ions in MgO by Thermal Conductivity Measurements," Proc. Roy. Soc. A 308 (1968), 355-376.

13. Casimir, H. B. G., Physica 5, 495 (1938).

14. Klemens, P. G., "Thermal Conductivity and Lattice Vibrational Modes," Solid State Phys., Vol. 7, Ed. F. Seitz, New York, Academic Press, 1958, pp. 1-98.

15. Slack, G. A., "Thermal Conductivity of MgO, Al_2O_3, $MgAl_2O_4$, and Fe_3O_4 Crystals From 3 to 300K". Phys. Rev., 126 (1962), 427-441.

16. Holland, M. G., "Analysis of Thermal Conductivity," Phys. Rev., 132 (1963), 2461-2471.

17. Pohl, R. O., "Localized Excitations in Solids," Ed. R. F. Wallis, New York, Plenum Press, 1968.

APPENDIX A

TABULATION OF DATA FOR THE SAMPLE

($KMgF_3:Cr^{2+}$)

2.6K to 28K

Temperature (K)	Thermal Conductivity (mW/cmK)
2.6	170.4
3.3	305.14
3.5	362.34
3.8	463.22
4.0	487.16
4.1	516.00
4.3	569.00
4.5	603.48
4.7	717.42
5.0	868.91
5.25	977.0
5.5	1049.0
5.6	1097.0
5.8	1124.4
5.9	1160.9
6.0	1235.8
6.1	1301.1
6.25	1359.5
6.4	1397.7
6.45	1440.0
6.6	1531.6
6.7	1591.5
6.85	1637.8
6.9	1708.6
7.05	1767.4
7.2	1807.2
7.3	1838.4
7.45	1936.1
7.65	2009.3
7.9	2120.9
8.0	2188.2
8.15	2324.9
8.2	2279.8

Temperature (K)	Thermal Conductivity (mW/cmK)
8.3	2215.6
8.4	2192.4
8.55	2498.9
8.7	2465.7
9.0	2604.1
9.2	2646.0
9.4	2726.0
9.7	2450.7
10.05	2626.5
10.15	2780.5
10.8	3005.1
11.9	2997.0
11.6	2814.0
12.0	3278.3
12.6	3459.9
15.4	3872.0
16.4	4149.6
17.2	4034.7
17.95	4247.9
18.9	4140.0
20.0	3790.0
24.0	2973.0
28.0	2299.8

APPENDIX B

ENERGY LEVELS OF THE GROUND STATE OF AN OCTAHEDRICALLY CO-ORDINATED $3d^4$ ION FROM THE JAHN-TELLER EFFECT MODEL OF FLETCHER AND STEVENS

For B > O.

B is the anharmonic constant can be positive or negative.

$$A_1 = -\frac{\delta}{3} - 2F_1D$$

$$A_2 = -\frac{\delta}{3} + 2F_1D$$

$$E_1 = \frac{\delta}{6} + \left(\frac{\delta^2}{4} + 2F_2^2D^2\right)^{\frac{1}{2}}$$

$$E_2 = \frac{\delta}{6} - \left(\frac{\delta^2}{4} + 2F_2^2D^2\right)^{\frac{1}{2}}$$

$$T_1 = -\frac{\delta}{3} - F_1D$$

$$T_2 = \frac{\delta}{6} + F_1\frac{D}{2} + \left\{\frac{(\delta-F_1D)^2}{4} + F_2^2D^2\right\}^{\frac{1}{2}}$$

$$T_2' = \frac{\delta}{6} + F_1\frac{D}{2}\left\{\frac{(\delta-F_1D)^2}{4} + F_2^2D^2\right\}^{\frac{1}{2}}$$

F_1 and F_2 are factors taht arise from thespin degeneracy. They are slowly function of δ, and were determined and tabulated by Fletcher and Stevens (5). In this work values of $F_1 = 1.0$ and $F_2 = 1.2$ were used. These are appropriate to the large value of δ required by the data.

VALUES OF ENERGY LEVELS IN cm^{-1} FROM THE FLETCHER AND STEVENS MODEL AS OBTAINED BY LÓPEZ

δ	D	A_1	T_1	E_2	T_2'	A_2	T_2	E_1
10.67	0.93	-5.4	-4.5	-3.8	-2.7	-1.7	7.2	7.3

VITA

Hadi Salamati-Mashhad

Candidate for the Degree of

Master of Science

Thesis: LOW TEMPERATURE THERMAL CONDUCTIVITY OF LIGHTLY DOPED $KMgF_3:Cr^{2+}$

Major Field: Physics

Biographical:

Personal Data: Born in Mashhad-Iran, Sept. 11, 1948, the son of Mr. and Mrs. M. K. Salamati.

Education: Graduated from University of Mashhad-Iran in September, 1972. Completed requirements for the Master of Science degree at Oklahoma State University in July, 1977.

Professional Experience: Graduate Teaching Assistant, Oklahoma State University, 1975-77.

Organization: Member of Sigma Pi Sigma.